REPORT DOCUMENTATION PAGE

Form Approved
OMB No. 0704-0188

Public reporting burden for this collection of information is estimated to average 1 hour per response, including the time for reviewing instructions, searching existing data sources, gathering and maintaining the data needed, and completing and reviewing the collection of information. Send comments regarding this burden estimate or any other aspect of this collection of information, including suggestions for reducing this burden, to Washington Headquarters Services, Directorate for Information Operations and Reports, 1215 Jefferson Davis Highway, Suite 1204, Arlington, VA 22202-4302, and to the Office of Management and Budget, Paperwork Reduction Project (0704-0188), Washington, DC 20503.

1. AGENCY USE ONLY (Leave blank)

2. REPORT DATE

3. REPORT TYPE AND DATES COVERED
FINAL REPORT 1 Dec 92 - 31 Mar 96

4. TITLE AND SUBTITLE
Arsenic Cluster Engineering

5. FUNDING NUMBERS
61102F
2305/BS

6. AUTHOR(S)
Professor Michael R. Melloch

7. PERFORMING ORGANIZATION NAME(S) AND ADDRESS(ES)
School of Electrical and Computer Engineering
Purdue University
1285 Electrical Engineering Building
West Lafayette, IN 47907-1285

8. PERFORMING ORGANIZATION
AFOSR-TR-96
0296

9. SPONSORING/MONITORING AGENCY NAME(S) AND ADDRESS(ES)
AFOSR/NE
110 Duncan Avenue Suite B115
Bolling AFB DC 20332-0001

10. SPONSORING/MONITORING AGENCY REPORT NUMBER
F49620-93-1-0031

11. SUPPLEMENTARY NOTES

19960618 064

12a. DISTRIBUTION/AVAILABILITY STATEMENT

APPROVED FOR PUBLIC RELEASE: DISTRIBUTION UNLIMITED

DTIC QUALITY INSPECTED 4

13. ABSTRACT (Maximum 200 words)

During this project we have refined our ability to "arsenic cluster engineer." We have demonstrated the ability to routinely control the density and diameters of the As clusters using the substrate temperature during MBE to set the excess As concentration and the subsequent coarsening anneal. We have shown that one can vary the incorporation of excess As in GaAs and AlGaAs epilayers by growing at low substrate temperatures using As4 and switching between MBE and MEE modes of growth. Upon anneal, the excess As precipitates preferentially in the GaAs regions of AlGaAs/GaAs heterojunctions due to the lower interfacial energy of an As cluster to GaAs matrix than that of an As cluster to AlGaAs matrix. The excess As can be retained in the AlGaAs regions where it will precipitate with anneal if thin AlAs As-diffusion barriers are used to clad the AlGaAs regions. These ACE tools will be very useful as we further explore the large electro-optic effect we have discovered in these composites.

15. NUMBER OF PAGES

16. PRICE CODE

17. SECURITY CLASSIFICATION OF REPORT	18. SECURITY CLASSIFICATION OF THIS PAGE	19. SECURITY CLASSIFICATION OF ABSTRACT	20. LIMITATION OF ABSTRACT
UNCLASSIFIED	UNCLASSIFIED	UNCLASSIFIED	

Final Technical Report on

Arsenic Cluster Engineering

AFOSR Grant F49620-93-1-0031

May 1996

M.R. Melloch
School of Electrical and Computer Engineering
Purdue University
West Lafayette, IN 47907-1285

Table of Contents

1. Introduction 3

2. Control of Composite Structures 3

3. Positioning of Arsenic Clusters in Superlattices 4

4. Excitonic Properties 5

5. Characterization of Doped LTG-GaAs 12

6. Summary 22

References 23

List Of Publications Acknowledging Support from this Contract 25

1. Introduction

Under normal molecular beam epitaxy (MBE) conditions, substrate temperatures in the neighborhood of 600 °C are typically used to grow high-quality, highly-stoichiometric GaAs. When GaAs is grown at low substrate temperatures—200 °C to 250 °C—the epilayer contains about 1.5% excess As and is highly strained[1,2] because of the excess As in the form of antisites and interstitials. Upon heating to 600 °C, which occurs when one grows structures using conventional MBE conditions on top of a low temperature grown (LTG) GaAs buffer, most of the strain is relaxed.[2] We discovered that this relaxing of the strain is accompanied by the excess As precipitating.[3] We will refer to this annealed LTG-GaAs material containing As precipitates (or clusters) as GaAs:As.

After our discovery of the existence of As precipitates in these materials, we proposed a model based on the As precipitates acting as internal Schottky barriers[4] to explain the semi-insulating properties of GaAs:As. Around each As precipitate is a depletion region. If the As precipitates are spaced close enough so that their depletion regions overlap, the material will be semi-insulating.

Excess As can also be incorporated into other III-V materials by MBE at low substrate temperatures such as AlGaAs; upon annealing LTG-AlGaAs this excess As also precipitates.[5,6] For AlGaAs/GaAs heterostructures grown at low substrate temperatures and subsequently annealed, we have observed that the As precipitates form preferentially in the GaAs regions.[6,7] We have used this phenomenon to form high density planes of As precipitates.[7] This preferential coarsening of the As clusters to the GaAs regions is because the interfacial energy of an As precipitate in contact with GaAs is smaller than for an As precipitate in contact with AlGaAs.[7]

Recently, we observed a very interesting phenomenon in GaAs:As—a large electro-optic effect at room-temperature for photon energies close to the bandgap. For AlGaAs:As a differential transmission of 60% with applied dc bias was obtained.[8] This is as large an effect as seen in multiple quantum well structures that are used for self electro-optic effect devices (SEEDs).[9] Therefore GaAs:As is potentially a very important material for electro-optic device applications.

The purpose of this research was to refine our ability to do Arsenic Cluster Engineering (ACE). This ability to do ACE is directly applicable to devices such as optical modulators and holographic memories that use the large electro-optic effect we have discovered in GaAs:As, high-speed photoconductors using the short carrier life-time in GaAs:As, and long wavelength optical detectors using the internal photoemission from the As precipitates.

2. Control of Composite Structures

An important component of ACE is the ability to control the final As cluster density and average cluster size. In this section we describe our development of the ability to do this.

The samples used in this work were grown by MBE in a modular Varian GEN II system. Normal MBE conditions were used except for the substrate temperature. Substrate temperatures ranging from 250 °C to 320 °C were used to set the amount of excess As in the epilayers. The As

flux was the dimer As_2, which incorporates As more efficiently than the tetramer As_4.[10] Two GaAs epilayers were grown, one with 0.3% excess As and one with 0.9% excess As. One $Al_{0.25}Ga_{0.75}As$ epilayer was grown with 0.2% excess As. Growth rates were 1 μm/h for all layers with excess As, and the group III to group IV beam equivalent pressure ratio was 20 as measured with an ion gauge in the substrate growth position. These non-stoichiometric epilayers were 1 μm thick and they were grown on thin AlAs layers. The AlAs layers allow the epilayers to be removed from the substrate by a selective etch so that the composites could be placed on transparent glass slides for transmission measurements, which are discussed in section 4.[11-13] The final composite structures were formed using rapid thermal processing (RTP) in an AG Associates Mini-Pulse system. The substrates were cleaved into approximately 1cm x 1cm samples and placed in the RTP with a GaAs proximity cap. The atmosphere in the RTP was nitrogen and all anneals were performed for 30s. The anneal temperatures ranged from 650 °C to 950 °C. Pieces were examined with cross-sectional transmission electron microscopy (TEM) using a JEM 2000 EX electron microscope. The resulting composite structures, as determined with TEM, are shown in fig. 1.

Observed in fig. 1 is that as one anneals GaAs:As at higher temperatures considerable precipitate coarsening occurs without a measurable change in the amount of As in precipitates. This coarsening occurs because the total energy of these two-phase systems is reduced by an increase in size and hence decrease in density of the clusters because of the reduction in total precipitate to matrix interfacial area. Such a coarsening process was first described by Ostwald and is referred to as Ostwald ripening.[14] For a given amount of excess As, the average diameter and density of the As clusters cannot be controlled independently. However the substrate temperature during MBE can be used to set the amount of excess As in the epilayer[5] and with the subsequent coarsening anneal any desired composite structure obtained. Therefore we accomplished a major goal of this program—we can readily control the composite structure with substrate temperature during MBE and the subsequent coarsening anneal—as illustrated in Fig 1.

3. Positioning of Arsenic Clusters in Superlattices

Another important component of ACE is the control of the positioning of As clusters in superlattices so that they form either in the GaAs well regions or the AlGaAs barrier regions. In this section we describe the tools we have developed for accomplishing this goal.

Several film structures were grown for this study. The epilayers were grown on two-inch diameter semi-insulating (100) GaAs substrates. Epilayers were grown using both the dimer As_2 and the tetramer As_4 as the arsenic flux. The As_2 (As_4) to Ga beam equivalent pressure used was 20 (18). Initially a GaAs buffer layer was grown at a normal substrate temperature of 600 °C and a growth rate of 1 μm/h. While continuing to grow GaAs, the substrate temperature was lowered to 260 °C. This took about 15 minutes resulting in a 0.25 μm GaAs temperature transition region.

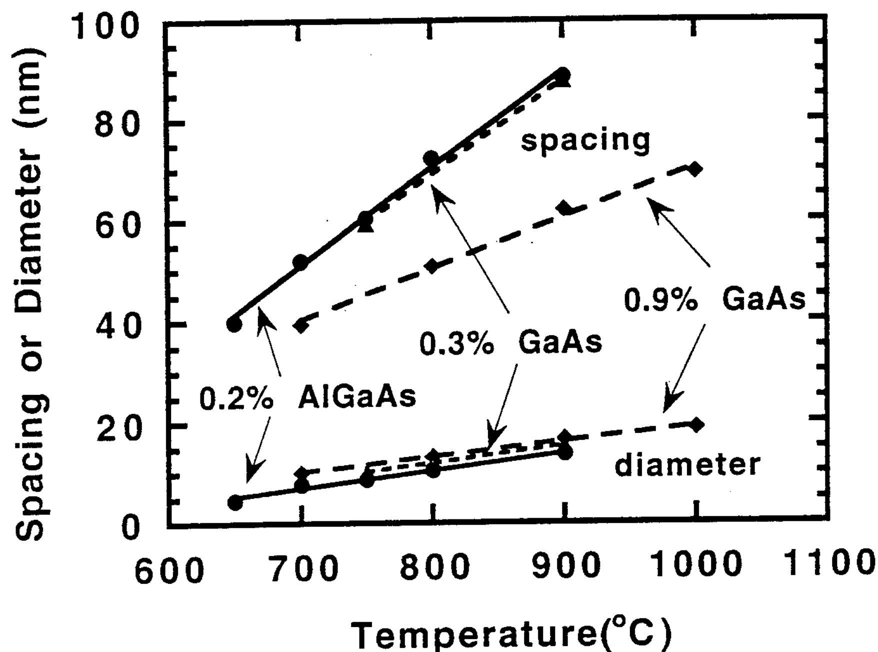

Fig. 1 Density and average size of As clusters in three different epilayers as a function of temperature for a 30 s anneal. Two of the epilayers are GaAs, one containing 0.3% excess As and the other 0.9% excess As. The third epilayer is $Al_{0.25}Ga_{0.75}As$ containing 0.2% excess As.

This was followed by the growth of quantum well structures. The GaAs wells were grown by migration enhanced epitaxy (MEE). MEE consists of separately supplying the group III and group V atoms to the growing III-V surface.[15] The enhanced migration of the group III atoms on the group-III stabilized surface allows for growth of high-quality, and hence highly-stoichiometric, GaAs at substrate temperatures down to 200 °C. The shutter sequence used for growing the MEE-GaAs well was 1s of Ga exposure, a 1s pause, a 1s As_4 (or As_2) exposure, and a 1s pause. The $Al_{0.2}Ga_{0.8}As$ barriers were grown at a rate of 1.2 µm/h by MBE and hence have a large excess of As. To keep the excess As in the AlGaAs barriers, they were clad by AlAs layers that were also grown by MEE so as not to contain excess As. (The effectiveness of AlAs as an As diffusion barrier was demonstrated by Yin et al.[16] who used a 20 nm AlAs layer between the n-GaAs channel of a transistor and a 50nm top GaAs epilayer with excess As. The purpose of the top 50nm GaAs epilayer with excess As was to improve the transistor breakdown voltage. In transistor structures without the AlAs As-diffusion barrier Yin et al.[16] observed complete compensation of the transistor's n-GaAs channel due to diffusion of excess As from the top GaAs epilayer while no compensation of the channel occurred in structures with the AlAs barrier.) After film growth, the

wafers were cleaved and samples annealed for 30s at temperatures ranging from 600 °C to 800 °C to cause precipitation of the excess As and subsequent coarsening of the As clusters.

The samples were examined by TEM. Shown in Fig. 2 is a TEM image of a sample grown using As_4. The GaAs wells and $Al_{0.2}Ga_{0.8}As$ barriers were 10 nm thick with 6 nm (lower region) or 12 nm (upper region) AlAs diffusion barriers. These AlAs layers appear as bright lines in Fig.2. The Fig. 2 sample was annealed for 30s at 800 °C. A large density of As clusters is observed in the $Al_{0.2}Ga_{0.8}As$ barriers while very few are observed in the GaAs wells and no As clusters are observed in the AlAs layers. This is the reverse of what is observed in a GaAs/$Al_{0.2}Ga_{0.8}As$ superlattice grown at low-temperatures by MBE and then annealed as shown in Fig. 3. In the Fig. 3 image the As clusters are all located in the GaAs wells with no clusters in the $Al_{0.2}Ga_{0.8}As$ barriers. Therefore the Fig. 2 image confirms that there is very little excess As in the GaAs well regions grown by MEE using As_4 and the 6 nm AlAs cladding layers are an effective As diffusion barrier. Another interesting observation in Fig. 2 is that the As clusters in the GaAs temperature transition region are as large as 20 nm in diameter whereas the As clusters in the AlGaAs regions are all about 10 nm in diameter. The AlAs layers cladding the $Al_{0.2}Ga_{0.8}As$ layers are constraining the As clusters to a diameter the width of the $Al_{0.2}Ga_{0.8}As$ layer because a cluster extending into the AlAs cladding layers would result in a substantial increase in interfacial energy. When a structure similar to Fig. 2 was grown but with 3 nm AlAs cladding layers, all the As clusters were found in the GaAs well regions with the $Al_{0.2}Ga_{0.8}As$ and AlAs regions free of precipitates. Apparently 3 nm AlAs regions are not sufficiently thick to provide a diffusion barrier to the excess As.

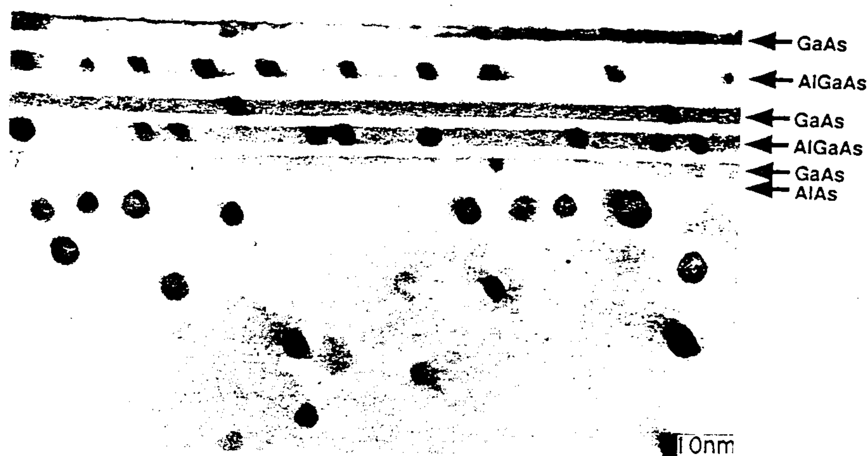

Fig. 2 TEM image of a film structure grown at 260°C using As_4. The bright lines are AlAs layers (the lowest one is marked) and were either 6nm or 12nm thick. The region below the marked AlAs layer is the GaAs temperature transition region. The three GaAs wells in the image are indicated with arrows. The AlAs layers and the GaAs regions between the AlAs layers were grown by MEE and as-grown are highly-stoichiometric. The $Al_{0.2}Ga_{0.8}As$ layers were grown by MBE and therefore as-grown have a large excess of As. A 30s 800°C anneal caused a precipitation of the excess As that remained in the AlGaAs regions due to the AlAs regions acting as As diffusion barriers.

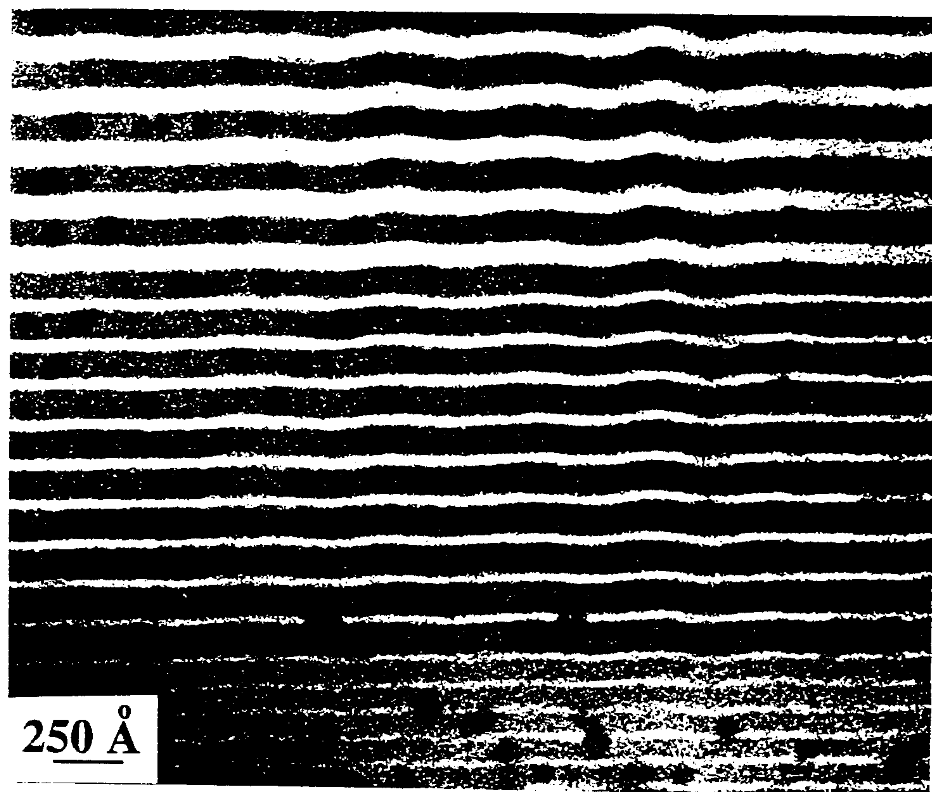

Fig. 3 TEM image of a GaAs/AlGaAs superlattice grown at 250°C by MBE and annealed to cause the excess As to precipitate. The AlGaAs regions appear as bright lines. The As clusters are all located in the GaAs regions due to the lower interfacial energy of an As cluster to GaAs matrix compared to an As cluster to AlGaAs matrix.

4. EXCITONIC PROPERTIES

Excitonic processes are especially sensitive to perturbations and therefore provide a convenient window with which to study microscopic material properties. GaAs:As and AlGaAs:As exhibit unusual electroabsorption for transition energies close to the excitonic transition. To measure the electroabsorption, after the precipitate anneal gold contacts were evaporated with a spacing of 1 mm and then the epilayers were removed and placed on glass slides. The band edge absorption is shown in fig. 4 as a function of applied electric field for the $Al_{0.25}Ga_{0.75}As$ epilayer containing As clusters and a high-quality, highly-stoichiometric GaAs epilayer. (Note the GaAs epilayer was implanted with protons at an energy of 160 keV and a dose of $1x10^{12}$ cm^{-2} to make it semi-insulating so that a field could be applied. This level of implantation has been shown to not adversely affect the excitonic properties of the GaAs epilayer.[17]) It is clear that the electro-optics of the composite is qualitatively very different from that of the stoichiometric material, indicating very different physics is controlling the electro-optic properties in these composites.

Shown in fig. 5 is the differential transmission for the AlGaAs epilayer with excess As for three different anneal temperatures and an applied electric field of 10 kV/cm. As the anneal temperature increases, the maximum differential transmission increases and then it begins to decrease with higher temperature anneals. The differential transmission is almost 60% for the sample annealed at 750 °C with an applied electric field of 10 kV/cm. In fig. 6 the differential transmission of the composite is compared to that of the quantum-confined Stark effect in a high-quality multiple quantum well sample. It is clear that the differential transmission of the composite has a broader bandwidth and is more sensitive to electric fields than the quantum-confined Stark effect in a multiple quantum well structure.

As further evidence that the As cluster spacing is controlling the electro-optic effect, the product of the oscillator strength and broadening for the three composites being discussed are shown in fig. 7. This figure of merit is plotted as a function of As cluster spacing in terms of the exciton's Bohr diameter, which is 23 nm in GaAs and 15 nm in AlGaAs. Clearly, the onset of the large electro-optic effect occurs when the As cluster spacing is about 3 exciton Bohr diameters in the material. When the As cluster spacing is less than about three exciton Bohr diameters, the clusters disrupt the exciton and there is not a large electro-optic effect. At a spacing of about three Bohr diameters there is a clear excitonic feature associated with the matrix material between the clusters. Without an applied field most of the As clusters are neutral. However, with an applied field, the clusters can become charged because of charge transfer between clusters. The resulting inhomogeneous internal microfields, which can be much larger than the applied electric field, cause a lifetime broadening of the exciton and cause the observed enhanced electro-optic effect. With further anneal and hence larger spacing between the As clusters, the composite looks more and more like stoichiometric material and the electro-optic effect approaches that of stoichiometric material.

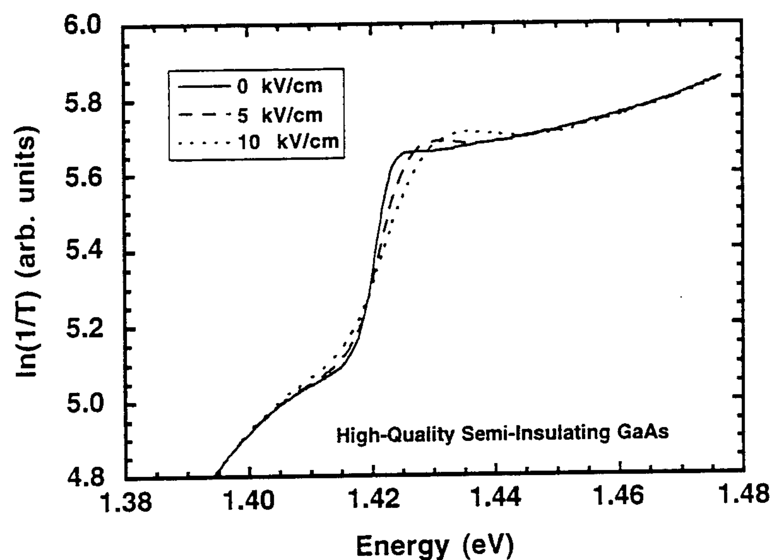

(a)

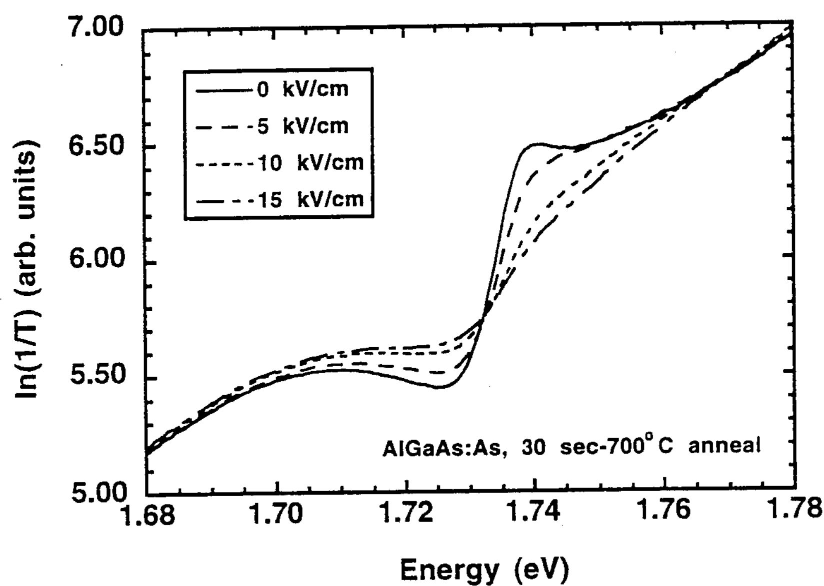

(b)

Fig. 4 Band edge absorption as a function of applied field for (a) high-quality, highly-stoichiometric GaAs and (b) $Al_{0.25}Ga_{0.75}As$ containing As clusters.

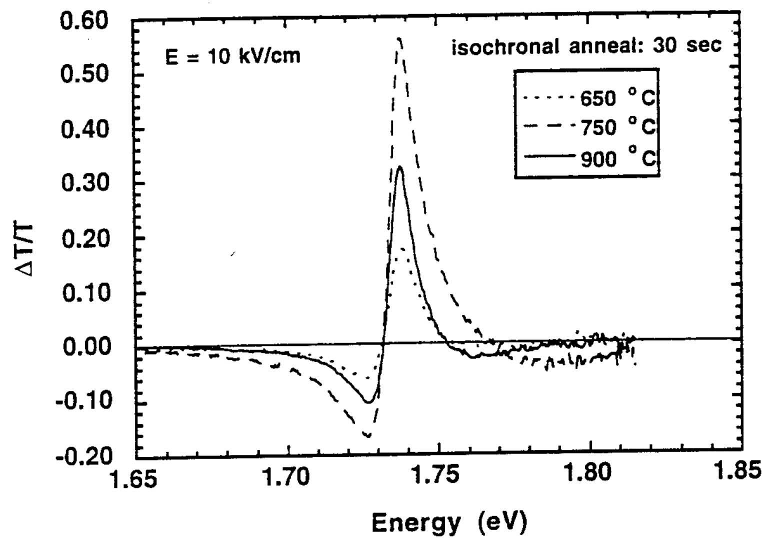

Fig. 5 Differential transmission as a function of coarsening anneal for a 1 μm thick $Al_{0.25}Ga_{0.75}As$ epilayer containing As clusters using an electric field of 10 kV/cm.

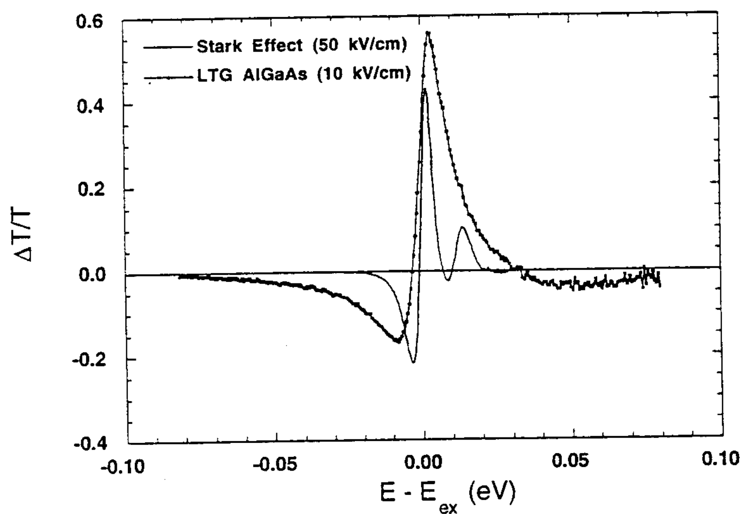

Fig. 6 Comparison of the quantum-confined Stark effect in a high-quality, highly-stoichiometric multiple-quantum well structure and in an AlGaAs epilayer containing As clusters.

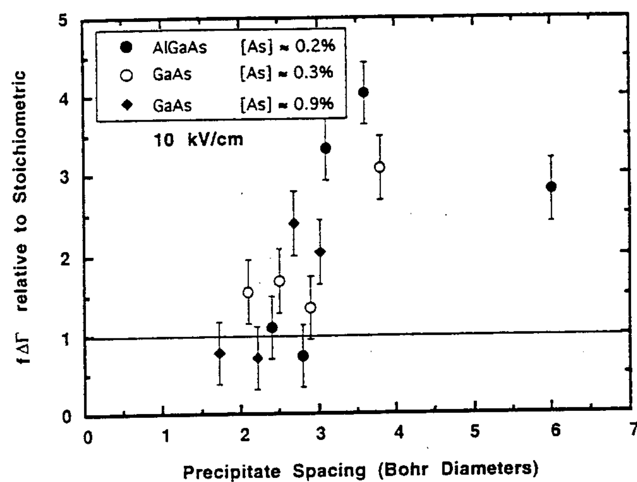

Fig. 7 Product of oscillator strength and lifetime broadening for three different epilayers as a function of As cluster spacing in Bohr diameters. Two of the epilayers are GaAs, one containing 0.3% excess As and the other 0.9% excess As. The third epilayer is $Al_{0.25}Ga_{0.75}As$ containing 0.2% excess As.

5. Characterization of Doped LTG-GaAs

As was shown in Section 2, post-growth anneal temperature can be used to control the size and density of arsenic precipitates in a GaAs matrix and the total amount of the excess arsenic in the epilayer is fixed by the substrate temperature during MBE.[5] We also performed a comprehensive study of another controlling factor we have over the structure of the arsenic precipitates—doping. It has been shown that delta-doping[18], p-n junctions[19], doping type[19,20,21], and doping concentration[19] can influence the coarsening of the arsenic precipitates. It has also been shown that as one anneals LTG Si-doped GaAs at higher temperatures, Hall measurements indicate an increase in electron concentration.[22] In our experiments we used a wide range of doping concentrations. The p-type epilayers were doped with Be to concentrations of $5x10^{17}$, $1x10^{18}$, $5x10^{18}$, $1x10^{19}$ and $5x10^{19}$ cm^{-3}. For the n-type epilayers, Si was the dopant and concentrations of $5x10^{17}$, $1x10^{18}$ and $5x10^{18}$ cm^{-3} were used.

Our objective in this study was to understand the nature of doped LTG-GaAs and to see how well the model of arsenic precipitates as buried Schottky barriers corroborates our results. In order to do so, our samples were annealed to temperatures of 700 °C, 800 °C, 900 °C and 1000 °C for 30s, yielding precipitates of various sizes. Detailed electrical and structural analyses were then performed. Hall measurements were made on the samples to observe how resistivity, carrier concentration and mobility vary with anneal temperature. TEM analysis on the corresponding samples yield average values for the diameters and the density of the clusters. Using the model proposed by Warren *et al.*[4] we are able to predict how the carrier concentration should change with anneal temperature. The Si-doped and Be-doped annealed LTG epilayers show very good agreement with the embedded Schottky barrier model. However, for the higher Be dopings, the carrier concentrations are lower than predicted by the embedded Schottky barrier model, indicating some compensation of the shallow acceptors by residual point defects.

Again the films used in our study were grown in our GEN II MBE system on 2 inch diameter undoped GaAs substrates. The substrates were degreased, etched for 1 min in a 60 °C solution of 5:1:1 H_2SO_4:H_2O_2:H_2O and placed in non-indium mounts. They were then loaded into a trolley and placed in the entry chamber of the MBE system where they were outgassed for 2h at 200 °C before being introduced into the buffer chamber of the MBE system. Liquid nitrogen was circulated through the radial vane and the cryoshrouds of the growth chamber starting 2h before film growth. The substrates were outgassed at 350 °C for 1h on a heater station in the buffer chamber immediately before being loaded into the growth chamber.

The arsenic source used was the dimer As_2, which has been reported to be more efficient than the tetramer source As_4 for arsenic incorporation in LTG-GaAs.[10] The growth rate was 1μm/h and the beam equivalent pressure of As_2 to Ga was 20. Initially 0.5 μm of undoped GaAs was grown at a substrate temperature of 600 °C. Growth was stopped and the substrate temperature lowered to 250 °C followed by the growth of a 0.75 μm uniformly doped LTG epilayer. A series of samples with Si concentrations of $5x10^{17}$, $1x10^{18}$, $5x10^{18}$ cm^{-3} and Be

concentrations of $5x10^{17}$, $1x10^{18}$, $5x10^{18}$, $1x10^{19}$, $5x10^{19}$ cm^{-3} were grown. The Be and Si concentrations were determined by Hall effect measurements on epilayers grown under normal growth conditions, that is with no excess arsenic in the epilayers. The Be-doped samples were then annealed with a proximity cap to 700 °C, 800 °C, and 900 °C for 30s using an AG Associates automated rapid thermal annealer (RTA). The Si-doped samples were annealed to the same temperatures as well as 1000 °C for 30s.

TEM analysis was performed on a few of the annealed samples to seek trends in the sizes and densities of the arsenic clusters with anneal temperature. [011] cross-sectional samples were prepared by the standard Ar ion thinning technique and examined using a JEM 2000EX electron microscope. Arsenic precipitates surrounded by a perfect GaAs crystal were observed in all the samples. Moiré fringes were also visible in the arsenic precipitates in all the samples. These indicate that the arsenic precipitates are crystalline in nature, even after a 1000 °C, 30s anneal. Quantitative analyses of the sizes and density of the arsenic precipitates were then carried out using (111) bright-field images. Sample thicknesses and subsequently volumes were determined from thickness contours. Cluster densities were calculated by counting the number of precipitates in a given volume. A few of the precipitates did not possess well-defined boundaries, but other contrasting factors such as density, atomic number, structure factor, moiré fringes and the lattice strain field around precipitates, aided in their identification. As a result, measured precipitate densities are very close to the actual values. Precipitate diameters were averaged over about 100 well-defined precipitates and the standard deviation, as a percent of the diameter, ranged from 15 to 30% of the average value.

The measured precipitate sizes and spacings are plotted versus anneal temperature in Fig. 8 for both the n- and p-doped material. The diameters of the precipitates ranged from about 50Å to 250Å. The precipitate densities ranged from $1x10^{15}$ to $1x10^{17}$ cm^{-3}. The spacing between precipitates (calculated from the density) ranged from about 200Å to 1000Å. It is clear that the arsenic clusters are coarsening with higher anneal temperatures. The volume fraction of excess arsenic, determined by TEM, was about 0.9% for the Si-doped material and about 0.6% for the Be-doped material, for all the different anneals. X-ray diffraction on a few of the annealed and as-grown materials was performed and the results of x-ray rocking curves showed no visible strain in the annealed material, indicating that most of the excess arsenic was precipitated by the 700°C, 30s anneal. The as-grown material did exhibit considerable strain, equating to a peak separation of about 130 arcseconds for the n-type material. At this point, it has not been determined why there is a difference in volume fraction of excess arsenic between the Si and Be-doped epilayers. It may be due to the surface atomic processes that are taking place during MBE.

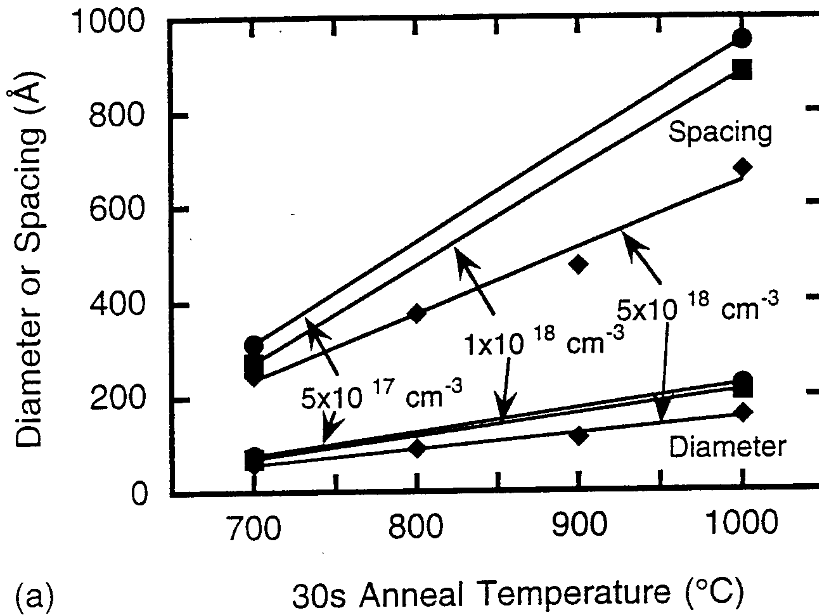

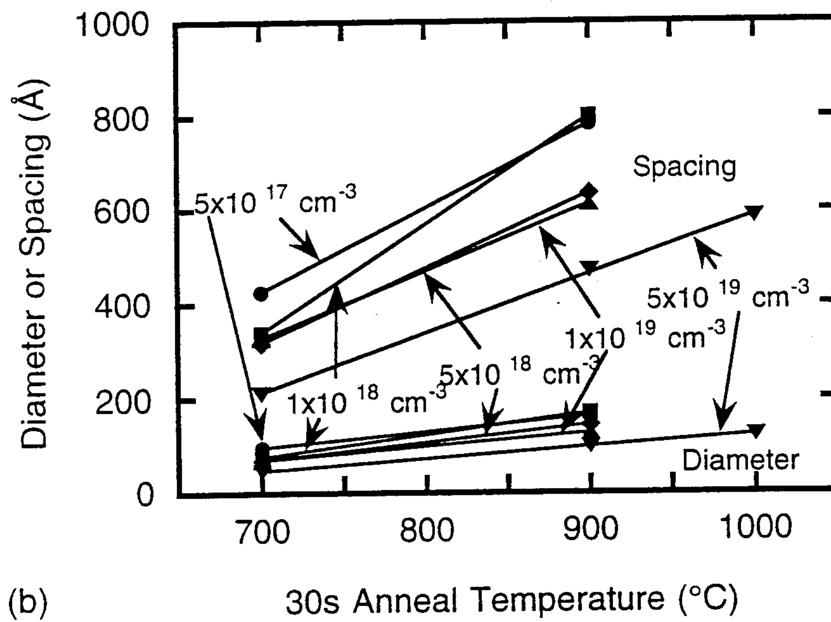

Fig. 8 Average cluster sizes and spacings as a function of anneal temperature for 30s isochronal anneals of LTG-GaAs epilayers for (a) three different Si-doping levels and (b) five different Be-doping levels.

TEM analysis revealed another interesting trend — higher doping levels resulted in smaller and more densely packed precipitates for a given anneal (see Fig. 8). This result will be discussed further below.

Electrical measurements were performed using a standard Hall effect system. Van der Pauw samples with In contacts were used. For the annealed LTG-GaAs epilayers, the In contacts were alloyed at 400 °C for about 30 seconds to provide good Ohmic contacts. The alloying temperature for the as-grown samples was 200 °C (less than the growth temperature) so as not to affect the samples. The electrical measurements are summarized in Tables I and II.

Fig. 9 plots resistivity vs. anneal temperature for both the Si- and Be-doped samples. Annealing the samples to 700 °C for 30s results in high resistivity material due to the high concentration of arsenic precipitates, as determined with TEM, which depletes the epilayer of free carriers. Fig. 9 also shows that the resistivity goes down with higher temperature (800 °C to 1000 °C) anneals. This is consistent with the TEM analysis which shows the precipitates to be coarsening with higher temperature anneals. When the arsenic precipitates coarsen to the point that the depletion regions no longer overlap, the carrier concentration goes up rapidly and the material turns conducting. Resistivities as low as 2.6×10^{-3} Ω-cm are obtained. Electrical measurements of the high resistivity samples shown in Fig. 9 are limited by substrate conduction. Also note that what appears to be an anneal temperature of 250 °C is just the growth temperature and those points represent the resistivity of the as-grown material.

The carrier concentrations and mobilities—as determined from Hall measurements—are shown in Fig. 10 and 11 respectively. Fig. 10 shows that carrier concentration increases with higher temperature anneals confirming the fact that the coarsening of the precipitates causes the depletion regions to no longer overlap and allow plenty of free carrier motion. This effect is also observed in Fig. 11, which shows that the mobility of the carriers increases with higher temperature anneals and mobilities as high as 1669 cm^2/V-sec are obtained. (Note that mobilities that look like zero in Fig. 11 are actually in the range from 1 to 15 cm^2/V-sec.) Mobility data for the Be-doped material is not plotted since some of the mobilities were so low that accurate Hall measurements were not possible. This also explains the fewer data points in Fig. 10(b). Also seen in Fig. 10(b) is the occurrence of n-type conductivity for the as-grown and some of the lower temperature annealed material; similar observations have been reported by others.[23,24]

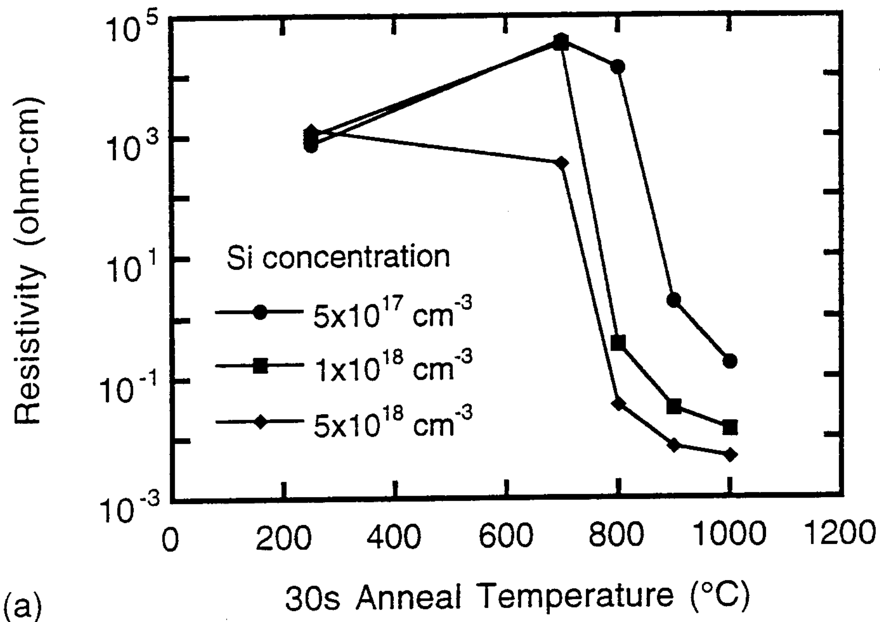

(a)

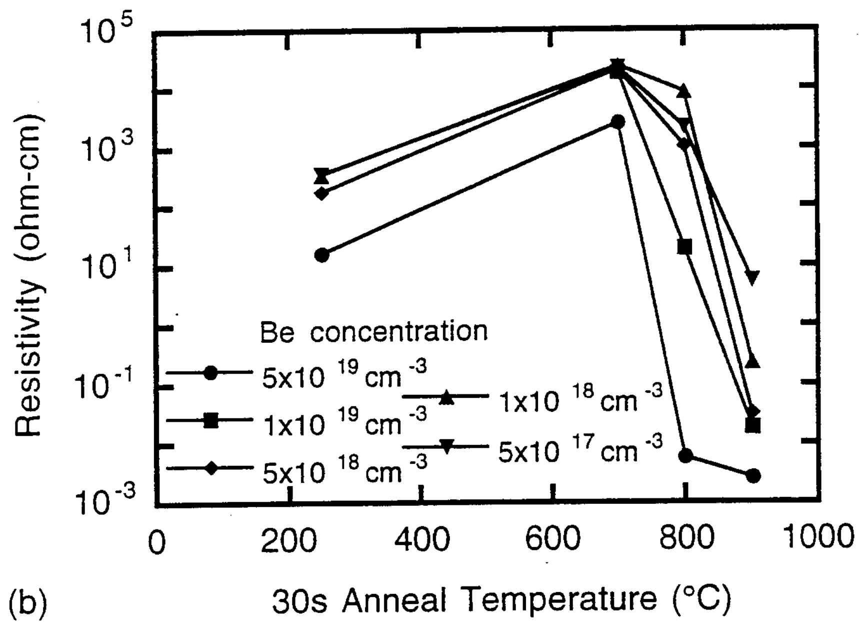

(b)

Fig. 9 Resistivity as a function of anneal temperature for 30s isochronal anneals of LTG-GaAs epilayers for (a) three different Si doping levels and (b) five different Be doping levels.

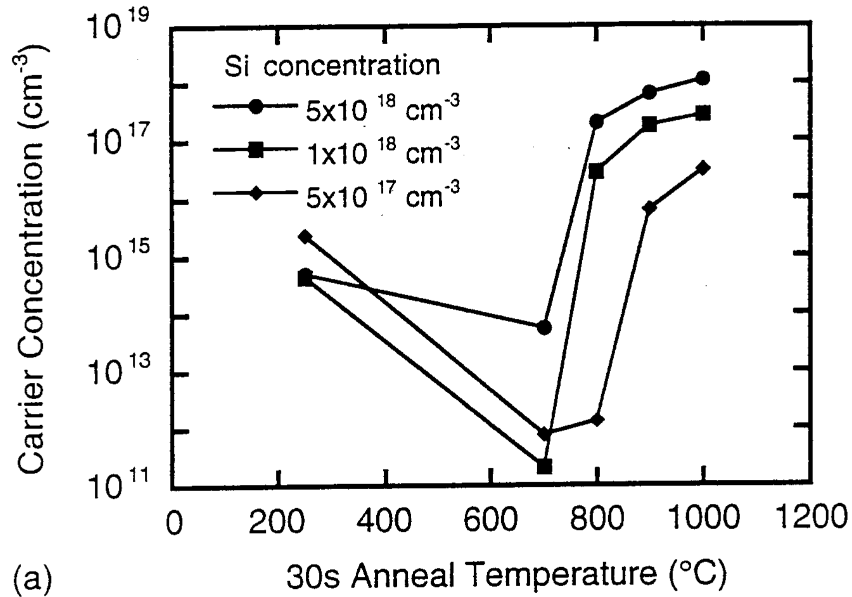

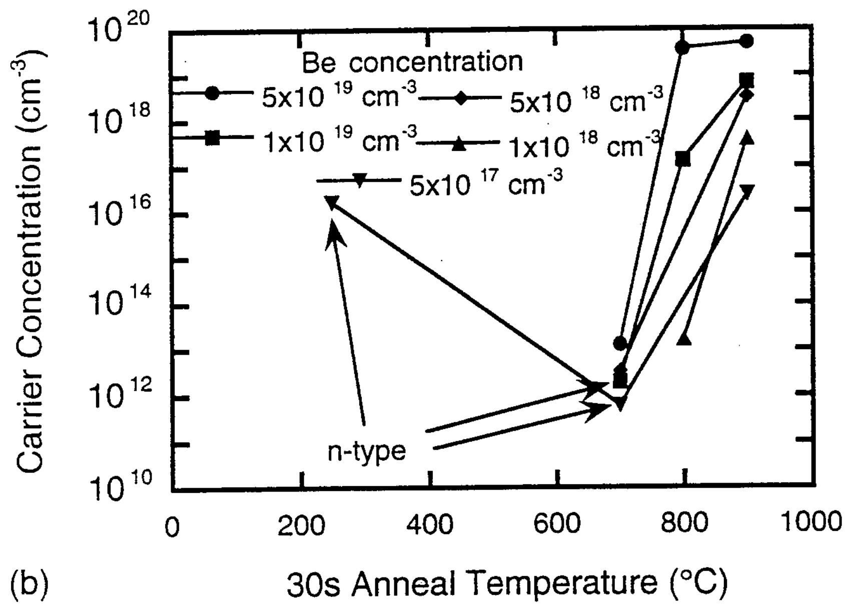

Fig. 10 Carrier concentration as a function of anneal temperature for 30s isochronal anneals of LTG-GaAs epilayers for (a) three different Si doping levels and (b) five different Be doping levels.

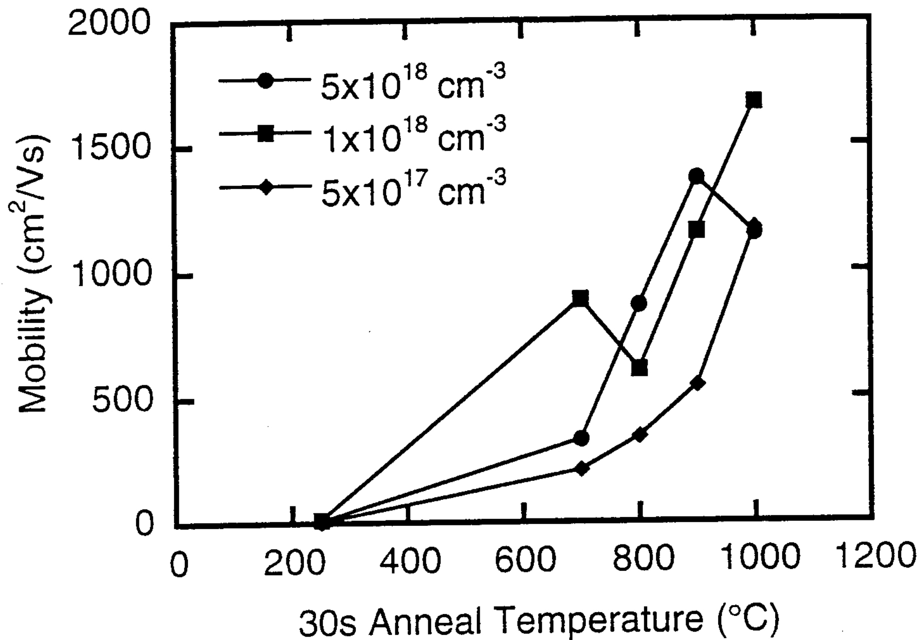

Fig. 11 Mobility as a function of anneal temperature for 30s isochronal anneals for the Si-doped LTG-GaAs epilayers.

From photoreflectance[22], STM[25], and photoemission[26] spectroscopy, the arsenic precipitate to GaAs Schottky barrier height, ϕ_B, has been measured to be 0.7 eV. Fig. 12 shows the model and band structure of an arsenic precipitate surrounded by its spherical depletion region. In this model the arsenic precipitate forms a Schottky barrier with the GaAs matrix analogous to a planar Schottky barrier. By solving Poisson's equation, the built-in potential V_o in Fig. 12—determined from the doping level of the material—is related to the arsenic precipitate radius r_o and the depletion radius r_s by,[4]

$$V_o = - (qN_D / 6\varepsilon) [(2r_s^3/r_o) + r_o^2 - 3r_s^2] , \qquad (1)$$

where N_D is the doping density and ε is the permittivity of the semiconductor matrix. This equation allows the calculation of the depletion radius for each of our samples, which enables an estimation of the free carrier concentration from the fraction of material depleted. The expected free carrier

concentration N_f for each sample is related to the doping density N_D, the depletion radius r_s, and the distance between precipitates d by

$$N_f = N_D [1 - (2r_s / d)^3] . \qquad (2)$$

Plotted in Fig. 13 is normalized free carrier concentration N_f / N_D vs. degree of depletion. Degree of depletion is the extent of the depletion region overlap and is given by $(2r_s) / d$ where d is the spacing between precipitates. A degree of depletion of 1 means the depletion regions are touching and a degree of depletion of 0.5 means only half the distance between precipitates is depleted. The theoretical curve calculated using (1) and (2) is illustrated by the solid curve in Fig. 13. The experimental free carrier concentrations (from Hall measurements) assumes conduction through the entire volume of each sample. However, when some of the material is depleted by arsenic precipitates, the volume available for conduction is less, and so actual carrier concentrations are higher in the undepleted regions. The experimental data points are scattered very close to the theoretical curve in Fig. 13(a) for the Si-doped material, indicating that the embedded Schottky barrier model accounts for the observed results. The existence of a few experimental data points to the right of a degree of depletion of 1, in Fig. 13(a), is due to our use of the depletion approximation in (1) and because there is still some contribution of carriers from unpinched off material not accounted for in (2).

The normalized hole concentrations as a function of depletion overlap are shown in Fig. 13(b). The 5×10^{17} cm^{-3} Be doped sample follows the predictions of the embedded Schottky barrier model (solid curve) but as the Be doping concentration increases, the experimental normalized hole concentrations shift to the left of the theoretical curve. This result is expected based on previous observations of arsenic precipitation in p-doped LTG-GaAs.[19] As-grown p-doped LTG-GaAs is at a lower free energy than as-grown n-doped LTG-GaAs because the excess arsenic, in the form of deep donor arsenic antisites, will compensate the p-doped LTG-GaAs. Therefore in p-type LTG-GaAs the excess arsenic does not precipitate as readily as in n-doped LTG-GaAs. Also, the higher the p-doping concentration the less readily does the arsenic precipitate, because a larger fraction of the arsenic antisites are ionized and compensating the shallow p-dopants. Furthermore, for a given anneal temperature, as the n- or p-doping concentration increases the arsenic clusters are smaller and denser, as seen in Fig. 8. This is due to the crystal trying to minimize its free energy by driving the Fermi level to midgap, which requires a higher arsenic precipitate density as the doping increases.

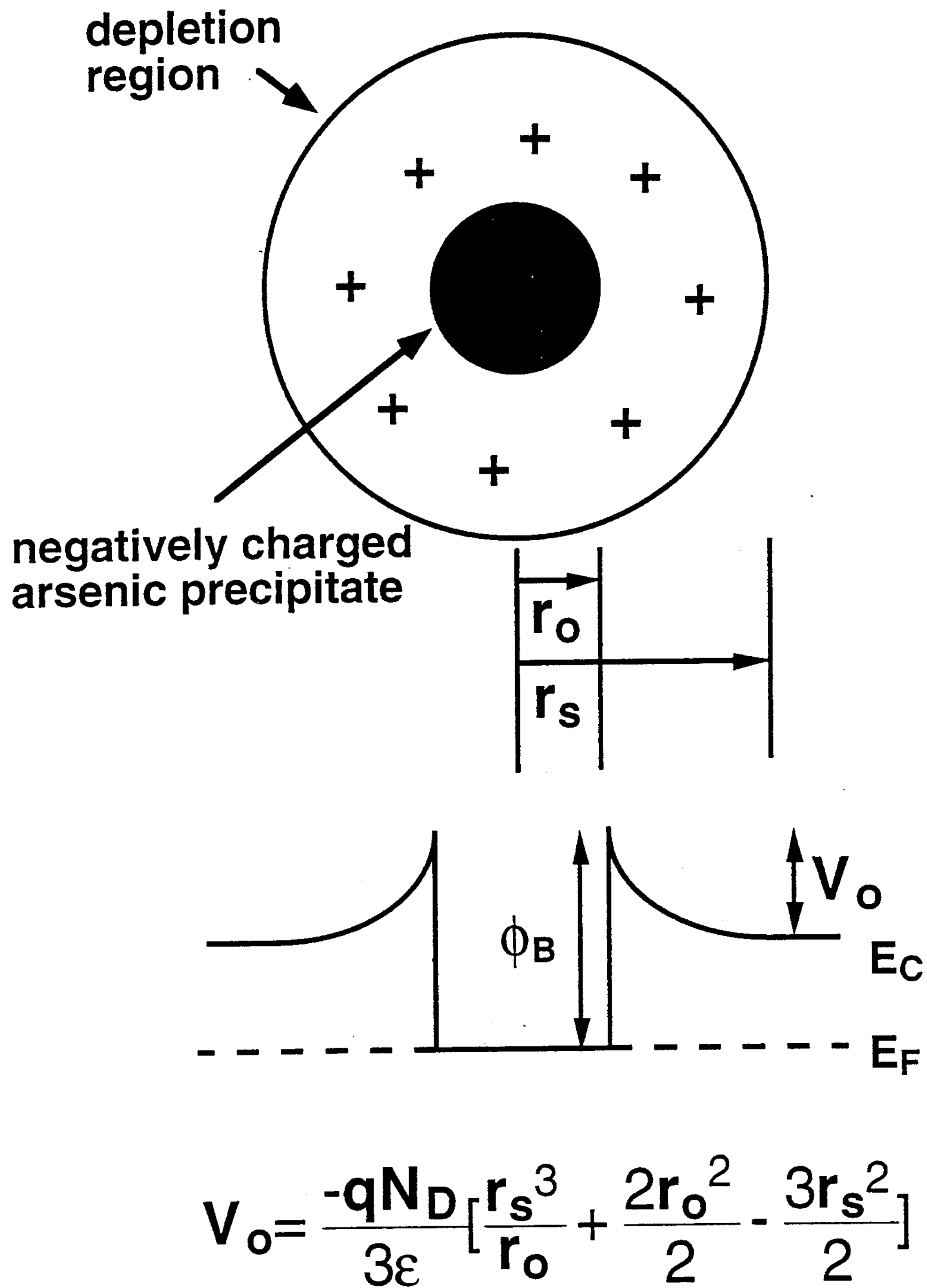

$$V_o = \frac{-qN_D}{3\varepsilon}\left[\frac{r_s^3}{r_o} + \frac{2r_o^2}{2} - \frac{3r_s^2}{2}\right]$$

Fig. 12 Schottky barrier model proposed by Warren *et al.*

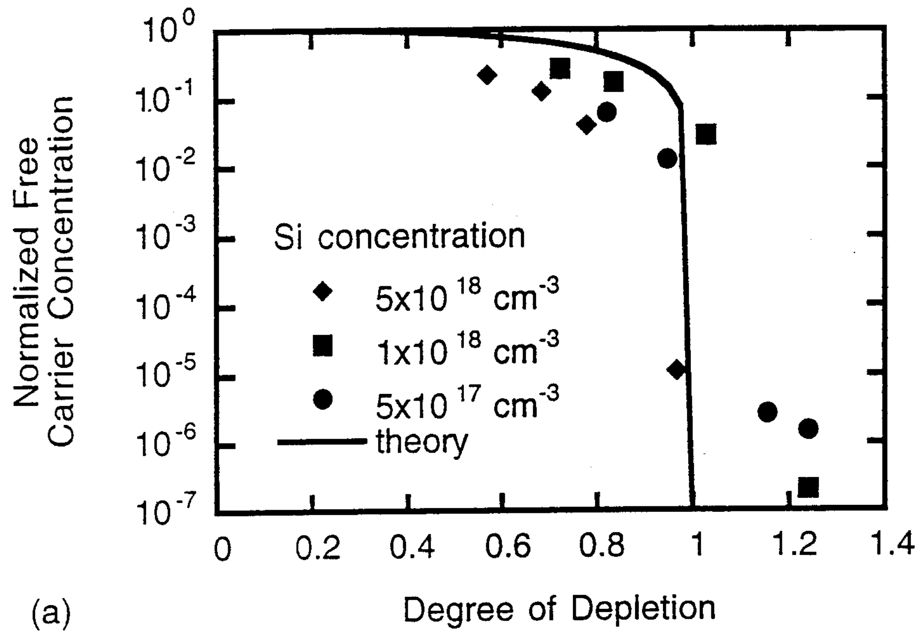

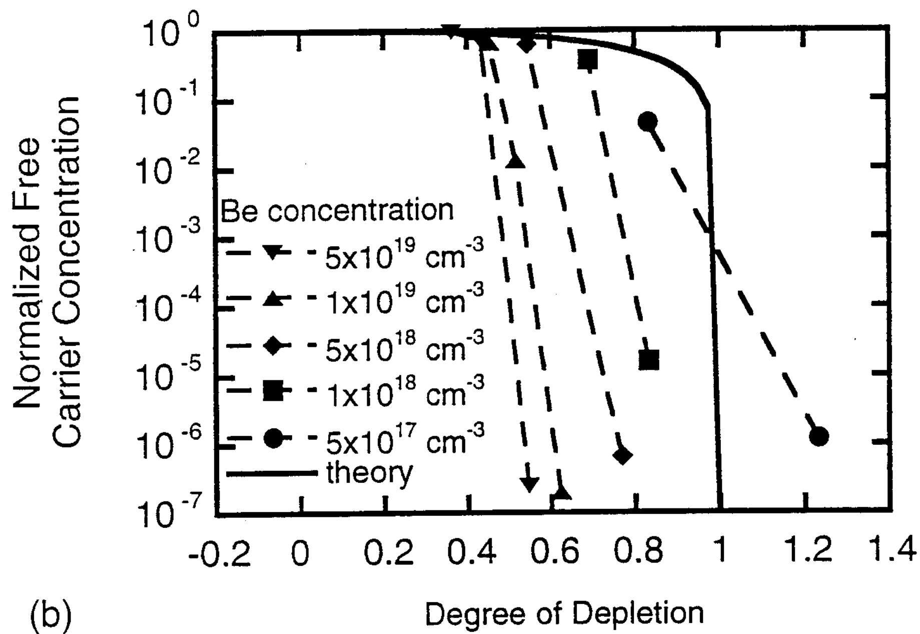

Fig. 13 Normalized carrier concentration versus degree of depletion for (a) three different Si doping levels and (b) five different Be doping levels. Degree of depletion is $2r_s$ / d where r_s is the depletion sphere radius and d is the distance between precipitates.

6. Summary

During this project we have refined our ability to "arsenic cluster engineer." We have demonstrated the ability to routinely control the density and diameters of the As clusters using the substrate temperature during MBE to set the excess As concentration and the subsequent coarsening anneal. We have shown that one can vary the incorporation of excess As in GaAs and AlGaAs epilayers by growing at low substrate temperatures using As4 and switching between MBE and MEE modes of growth. Upon anneal, the excess As precipitates preferentially in the GaAs regions of AlGaAs/GaAs heterojunctions due to the lower interfacial energy of an As cluster to GaAs matrix than that of an As cluster to AlGaAs matrix. The excess As can be retained in the AlGaAs regions where it will precipitate with anneal if thin AlAs As-diffusion barriers are used to clad the AlGaAs regions. These ACE tools will be very useful as we further explore the large electro-optic effect we have discovered in these composites.

The effect of anneal on the structure and electronic properties of n- and p-doped LTG-GaAs has also been studied. The electronic properties of the as-grown LTG-GaAs epilayers are controlled by point defects. As the material is annealed, the excess arsenic precipitates and plays an increased role in controlling the electronic properties of the material, whereas the role of point defects decreases. For sufficient anneal, the embedded Schottky barrier model for the arsenic precipitates adequately explains the electronic properties of annealed doped LTG-GaAs epilayers. With an anneal of 700 °C for 30s there is a large increase in the resistivity of the doped LTG-GaAs epilayers. This increase in resistivity is due to the arsenic precipitates depleting the GaAs matrix of free carriers. With higher anneals, the arsenic precipitates coarsen, the depletion regions surrounding the arsenic precipitates no longer overlap, and the conductivity approaches that expected from the n- or p-doping. For high Be concentrations there is some compensation of the shallow acceptors due to residual arsenic antisites, leading to depletion of the epilayer by the arsenic precipitates at lower arsenic precipitate concentrations than expected. Also, for a given anneal temperature, a higher n- or p-doping concentration results in a higher density and a smaller diameter for the arsenic precipitates due to the crystal minimizing its free energy.

REFERENCES

1. M. Kaminska, E.R. Weber, Z. Liliental-Weber, R. Leon, and Z.U. Rek, J. Vac. Sci. Technol. B7 (1989) 710.
2. R.J. Matyi, M.R. Melloch, and J.M. Woodall, Appl. Phys. Lett. 60 (1992) 2642.
3. M.R. Melloch, N. Otsuka, J.M. Woodall, A.C. Warren, and J.L. Freeouf, Appl. Phys. Lett. 57 (1990) 1531.
4. A.C. Warren, J.M. Woodall, J.L. Freeouf, D. Grischkowsky, D.T. McInturff, M.R. Melloch, and N. Otsuka, "Arsenic Precipitates and the Semi-Insulating Properties of GaAs Buffer Layers Grown by Low Temperature Molecular Beam Epitaxy," Appl. Phys. Lett. 57, 1331(1990).
5. K. Mahalingam, N. Otsuka, M.R. Melloch, J.M. Woodall, and A.C. Warren, "Substrate Temperature Dependence of Arsenic Precipitate Formation in AlGaAs and GaAs," Journal of Vac. Sci and Tech. B9, 2328(1991).
6. K. Mahalingam, N. Otsuka, M.R. Melloch, J.M. Woodall, and A.C. Warren, "Arsenic Precipitate Depletion and Accumulation Zones at AlGaAs/GaAs Heterojunctions Grown at Low Substrate Temperatures by Molecular Beam Epitaxy," J. of Vac. Sci. and Technol. B10, 812(1992).
7. K. Mahalingam, N. Otsuka, M.R. Melloch, and J.M. Woodall, "Arsenic Precipitates in $Al_{0.3}Ga_{0.7}As$/GaAs Multiple Superlattice and Quantum Well Structures," Appl. Phys. Lett. 60, 3253(1992).
8. M.R. Melloch, D.D. Nolte, N. Otsuka, C.L. Chang, and J.M. Woodall, "Arsenic Cluster Engineering for Excitonic Electro-Optics,"*J. of Vac. Sci. and Tech.*, B10, 795(1993).
9. D.A.B. Miller, OQE22, 561(1990).
10. M.R. Melloch, K. Mahalingam, N. Otsuka, J.M. Woodall, and A.C. Warren, "GaAs buffer layers grown at low substrate temperatures using As_2 and the formation of arsenic precipitates," *J. of Crys. Growth*, Vol. 111, pp. 39-42, 1991.
11. F. Stern and J.M. Woodall, "Photon recycling in semiconductor lasers," *J. Appl. Phys.*, Vol. 45, pp. 3904-3906, 1974.
12. E. Yablonovitch, T. Gmitter, J.P. Harbison, and R. Bhat, "Extreme selectivity in the lift-off of epitaxial GaAs films," *Appl. Phys. Lett.*, Vol. 51, pp. 2222-2224, December 28, 1987.
13. E. Yablonovitch, D.M. Hwang, T. Gmitter, L.T. Florez, and J.P. Harbison, "Van der Waals bonding of GaAs epitaxial liftoff films onto arbitrary substrates," *Appl. Phys. Lett.*, Vol. 56, pp. 2419-2421, June 11, 1990.
14. W. Ostwald, Z. Phys. Chem. 37 (1901) 385.
15. Yoshiji Horikoshi, Minoru Kawashima, and Hiroshi Yamaguchi, Jap. J. of Appl. Phys. 25 (1986) L868.
16. L.-W. Yin, Y. Hwang, J.H. Lee, R.M. Kolbas, R.J. Trew, and U.K. Mishra, IEEE Elec. Dev. Lett. EDL-11 (1990) 561.

17. Q. Wang, R.M. Brubaker, D.D. Nolte, and M.R. Melloch, "Photorefractive quantum wells: transverse Franz-Keldysh geometry," *J. of the Optical Soc. of America B*, Vol. 9, pp. 1626-1641, September 1992.
18. M.R. Melloch, N. Otsuka, K. Mahalingam, C.L. Chang, P.D. Kirchner, J.M. Woodall, and A.C. Warren, Appl. Phys. Lett. **61**, 177 (1992).
19. M.R. Melloch, N. Otsuka, K. Mahalingam, C.L. Chang, J.M. Woodall, G. D. Pettit, P.D. Kirchner, F. Cardone, A.C. Warren, and D.D. Nolte, J. Appl. Phys. **72**, 3509 (1992).
20. J.P. Ibbetson, J.S. Speck, A.C. Gossard, and U.K. Mishra, Appl. Phys. Lett. **62**, 169 (1993).
21. C.L. Chang, K. Mahalingam, N. Otsuka, M.R. Melloch, and J.M. Woodall, J. Elec. Mat. **22**, 1413 (1993).
22. A.C. Warren, J.M. Woodall, P.D. Kirchner, X. Yin, F. Pollak, M.R. Melloch, N. Otsuka, and K. Mahalingam, Phys. Rev. B **46**, 4617 (1992).
23. D.E. Bliss, W. Walukiewicz, J.W. Ager, III, E.E. Haller, K.T. Chan, and S. Tanigawa, J. Appl. Phys. **71**, 1699 (1992).
24. S. O'Hagan, and M. Missous, J. Appl. Phys. **75**, 7835 (1994).
25. R.M. Feenstra, A. Vaterlaus, J.M. Woodall, and G.D. Pettit, Appl. Phys. Lett. **63**, 2528 (1993).
26. D.T. McInturff, J.M. Woodall, A.C. Warren, N. Braslau, G.D. Pettit, P.D. Kirchner, and M.R. Melloch, Appl. Phys. Lett. **60**, 448 (1992).

List of Publications Acknowledging Support From this Contract

1. M.R. Melloch, C.L. Chang, N. Otsuka, K. Mahalingam, J.M. Woodall, and P.D. Kirchner, "Two-Dimensional Arsenic-Precipitate Structures In GaAs," Journal of Crystal Growth 127, 499(1993).
2. D.T. McInturff, J.M. Woodall, A.C. Warren, N. Braslou, G.D. Pettit, P.D. Kirchner, and M.R. Melloch, "Photoemission Spectroscopy of $Al_{0.27}Ga_{0.73}As$:As Photodiodes," Appl. Phys. Lett. 62, 2367(1993).
3. M.R. Melloch, D.D. Nolte, N. Otsuka, C.L. Chang, and J.M. Woodall, "Arsenic Cluster Engineering for Excitonic Electro-Optics," J. of Vac. Sci. and Tech. B10, 795(1993).
4. Lawrence Carin, David R. Kralj, Michael R. Melloch, and Jerry M. Woodall, "Characterization of Planar Antennas Fabricated on GaAs Epilayers Containing As Clusters For Picosecond Short-Pulse Applications," IEEE Microwave and Guided Wave Lett. 3, 339(1993).
5. E.S. Harmon, M.R. Melloch, J.M. Woodall, D.D. Nolte, N. Otsuka, and C.L. Chang, "Carrier Lifetime versus Anneal in Low Temperature Grown GaAs," Appl. Phys. Lett. 63, 2248(1993). Rooks, "1D-to-2D Tunneling in Electron Waveguides," Phys. Rev. B 48, 15057(1993).
6. C.L. Chang, K. Mahalingam, N. Otsuka, M.R. Melloch, and J.M. Woodall, "Precipitation of Arsenic in Doped GaAs," J. of Elec. Mats. 22, 1413(1993).
* 7. M.R. Melloch, J.M. Woodall, N. Otsuka, K. Mahalingam, C.L. Chang, D.D. Nolte, and G.D. Pettit, "GaAs, AlGaAs, and InGaAs Epilayers Containing As Clusters: Metal/Semiconductor Composites," Materials Science and Engineering B22, 31(1993) (INVITED).
8. Arifur Rahman, David Kralj, Sung Jin Hong, Lawrence Carin, Michael R. Melloch, and Jerry M. Woodall, "Photoconductively Switched Antennas for Measuring Target Resonances," Appl. Phys. Lett. 64, 2178(1994).
* 9. M.R. Melloch, N. Otsuka, E.S. Harmon, D.D. Nolte, J.M. Woodall, and D.T. McInturff, "Physics and Applications of Metallic Arsenic Clusters in GaAs Based Layer Structures," Japanese Journal of Appl. Phys 32, suppl. 32-3, 771(1994) (INVITED).
10. V. Mahadev, M.R. Melloch, J.M. Woodall, N. Otsuka, and G.L. Liedl, "Effect of Dopants on Arsenic Precipitation in GaAs Deposited at Low Temperatures," J. of Elec. Mat. 23, 1015(1994).
11. J.C.P. Chang, N. Otsuka, E.S. Harmon, M.R. Melloch, and J.M. Woodall, "Precipitation in Fe and Ni-Implanted and Annealed GaAs," Appl. Phys. Lett. 65, 2801(1994).
12. N. Atique, E.S. Harmon, J.C.P. Chang, J.M. Woodall, M.R. Melloch,and N. Otsuka, "Electrical and Structural Properties of Be- and Si-doped Low-Temperature-Grown GaAs," J. of Appl. Phys. 77, 1471(1995).
13. M.P. Patkar, T.P. Chin, J.M. Woodall, M.S. Lundstrom, and M.R. Melloch, "Very Low Resistance Non-Alloyed Ohmic Contacts Using Low Temperature Molecular Beam Epitaxy of GaAs," Appl. Phys. Lett. 66, 1412(1995).
14. I. Lahiri, D.D. Nolte, E.S. Harmon, M.R. Melloch, and J.M. Woodall, "Ultrafast-Lifeime Quantum Wells with Sharp Exciton Spectra," Appl. Phys. Lett. 66, 2519(1995).
15. E.S. Harmon, D.T. McInturff, M.R. Melloch, and J.M. Woodall, "Novel GaAs Photodetector with Gain for Long Wavelength Detection," J. of Vac. Sci. and Tech. B13, 768(1995).
16. I Lahiri, D.D. Nolte, J.C.P. Chang, J.M. Woodall, and M.R. Melloch, "The Role of Excess Arsenic in Interface Mixing in Low-Temperature-Grown AlAs/GaAs Superlattices," Appl. Phys. Lett. 67, 1244(1995).
17. I. Lahiri, K.M. Kwolak, D.D. Nolte, and M.R. Melloch, "Photorefractive p-i-n Diode Quantum Well Spatial Light Modulators," Appl. Phys. Lett. 67, 1408(1995).
18. J.C.P. Chang, J.M. Woodall, M.R. Melloch, I. Lahiri, D.D. Nolte, N.Y. Li, and C.W. Tu, "Investigation of Interace Intermixing and Roughening in Low-Temperature-Grown

AlAs/GaAs Multiple Quantum Wells During Thermal Annealing by Chemical Lattice Imaging and X-Ray Diffraction," Appl. Phys. Lett. 67, 3491(1995).

19. E.B. Cohen, D.B. Janes, K.J. Webb, J.N. Shenoy, J.M. Woodall, and M.R. Melloch, "A 2-DEG/Low-Temperature-Grown GaAs Dual Channel Heterostructure Transistor," Superlattices and Microstructures, 17, 345(1995).
20. I. Lahiri, María Aguilar, D.D. Nolte, and M.R. Melloch, "High-Efficiency Stark-Geometry Photorefractive Quantum Wells with Intrinsic Cladding Layers," Appl. Phys. Lett. 68, 517(1996).
21. E.H. Chen, D.T. McInturff, T.P. Chin, M.R. Melloch, and J.M. Woodall, "Use of Annealed Low-Temperature-Grown GaAs as a Selective Photoetch-Stop Layer," Appl. Phys. Lett. 68, 1678(1996).
22. A.J. Lochtefeld, M.R. Melloch, J.C.P. Chang and E.S. Harmon,, "The Role of Point Defects and Arsenic Precipitates in Carrier Trapping and Recombination in Low-Temperature Grown GaAs," submitted to Appl. Phys. Lett.
23. I. Lahiri, D.D. Nolte, M.R. Melloch, J.M. Woodall, and W. Walukiewicz, "Transient Enhanced Diffusion in Nonstoichiometric Quantum Wells and the Decay of Suptersaturated Vacancy Concentrations," submitted to Appl. Phys. Lett.
24. M.R. Melloch, I. Lahiri, D.D. Nolte, J.C.P. Chang, E.S. Harmon, J.M. Woodall, N.Y. Li, and C.W. Tu, "Molecular-Beam Epitaxy of High-Quality, Non-Stoichiometric Multiple Quantum Wells," submitted to the J. of Vac. Sci and Tech. B.